Chapter 7

Pyrolysis of Banana (*Musa balbisiana*) Trunk: Kinetics of Thermal Degradation Process

Abstract

The thermochemical characterization (proximate and ultimate analysis and higher heating value) of banana trunk biomass waste has been carried out. The thermo-gravimetric and differential scanning calorimetric (DSC) investigations have been made at four heating rates of 10, 15, 20 and 25^{o}C/min. The TGA data have been used to carry out kinetic analysis and evaluate the kinetic and thermodynamic parameters using iso-conversional models. The values of activation energy increase with conversion (α) irrespective of the iso-conversional model used. The average values of activation energies (E_{α}) are found to be 386.21, 355.43, 385.77, 355.01, 379.67, and 292.78kJ/mol for Flynn-wall-Ozawa (FWO), Starink, Kissinger-Akahira-Sunose (KAS), Tang, Vyzovkin and Vyzovkin AIC model, respectively. The average values of change in enthalpy, Gibbs free energy, and entropy have been calculated. The reaction mechanisms of pyrolysis have been predicted using Criado's method.

7.1 Introduction

Banana is the most widely grown fruity plant in the world. It is produced in Asia, Latin America, and Africa, each contributing around 50.82, 32.97 and 14.09%, respectively to the total world production. Europe (0.57%) and Oceania (1.55%) also contribute insignificant amounts. Some African countries, Brazil, China, Ecuador, India, and Philippines are the major banana producing countries. During 2010 to 2017, India produced on an average 29 million tonnes of banana, China around 11 million tonnes, Philippines around 7.5 million tonnes and Ecuador and Brazil each around 7 million tonnes. Colombia, Costa Rica, and Guatemala are other Latin American countries producing sizeable amount

of banana. The banana production area in the world has increased steadily from 3.6 million hectares in 1993 to 5.6 million hectares in 2017 (FAOSTAT, 2014). Between the years 2000 to 2017, the global production of banana increased at the compound annual rate of 3.2% reaching 114 million tonnes in 2017 from around 67 million tonnes in 2007. Banana is a tropical, herbaceous and perennial plant belonging to the Musaceae family, which produces a large flower cluster, bears fruits and then dies. The plant is cut to bring the crop down and harvest the fruits. The main stem (or pseudo-stem or trunk) of banana is a juicy cylindrical cluster of leaf stalk bases. The subterranean stem is known as corm and the part that supports fruits is known as peduncle, stalk or rachis. After harvesting the fruit all these portions become waste biomass. At the packaging and processing plant, the banana bunch rachis and damaged/rotten fruits also become additional residual biomass. The banana biomass waste production is to the tune of 220 tonnes per hectare (Padam et al., 2012). In addition to the plant biomass wastes, the rejected fruits that fail to meet the required quality standards may contribute between 8 and 20 percent of additional biomass waste. For every tone of banana produced, about 100 kg of fruit rejects and 4 tons of biomass waste comprising leaves, pseudo-stem, rotten fruits, fruit bunch stem and rhizomes are produced, totaling to approximately 4- times the banana fruit produce (Subayo and Chafidz, 2018).

The banana biomass waste thus generated is either left in the field or taken to open dumps. In both cases, the ligno-cellulosic biomass wastes produce greenhouse gases as they decompose. Thus it is seen that banana farming and processing generates thousands of tons of waste biomass, which is currently being improperly managed causing serious environmental problems (Padam et al., 2014). There is a need to evaluate the potential of

this huge biomass waste for utilization as a fuel or feedstock for biochemical and thermochemical conversion processes.

7.2 Biomass collection, sample preparation and thermo-chemical characterization

Collection and preparation of the banana trunk (BT) biomass sample was carried out as described earlier by Kumar et al. (2019c). The ASTM standard methods (E-871, E-872 and D-1102) were used for the determination of moisture, volatile matter, ash, and fixed carbon contents. The ultimate analysis (C, H, O, N, and S contents) was carried out using the CHNS Analyzer (Euro EA, Elemental Analyzer, Italy). The higher heating value (HHV in MJ/kg) was evaluated using a digital bomb calorimeter (Model no. RSB 3, Rajdhani Scientific, Delhi India). The functional groups of the organic compounds present in the biomass sample were detected with the help of a Fourier Transform Infrared (FTIR) spectroscope (5700 FTIR, Thermo-electron Cooperation, and Waltham, Massachusetts, United States). The hemicellulose, cellulose and lignin contents were evaluated employing the method of Soest et al (1991). The thermal degradation behaviour of the powder BT biomass sample was investigated using a thermo-gravimetric analysis unit (TGA- 50 00377, Shimadzu Corp. Kyoto, Japan). The TGA data were collected between the temperature ranges of ambient (30°C) to 800°C, at four different heating rates – 10, 15, 20 and 25°C/min. The TGA experiments were performed in nitrogen atmosphere (N_2 flow rate: 100 mL/min). The differentiation of TGA data was carried out to know the corresponding differential thermo-gravimetric (DTG) values using Origin Pro (Version 11) software. The heat flow (mW/mg) analysis at four heating rates was performed between 30 and 600 °C using a differential scanning calorimeter (DSC-60 Plus, Shimadzu Corp. Kyoto, Japan).

7.3. Results and discussion

7.3.1 Thermochemical characterization

The results of proximate and ultimate analyses, calorific value, and biological composition are listed in Table 7.1. The estimations of proximate analysis, bulk density and chemical composition were carried out in triplicate and average values with corresponding variations are reported in Table 1 together with published values of Nolasco et al. (1998), Guimarães et al. (2009), Sellin et al. (2013), Abdullah et al. (2014), de Oliveira Maia et al. (2014), Cheng et al. (2016), Kabenge et al. (2018), Kumar et al. (2019) and Selvarajoo et al. (2019). The bulk density of the raw BT sample was found to be 161.3kg/m^3. It influences the thermal degradation of biomass sample; thusly kinetic parameters (Kumar et al., 2019b). The moisture content was found to be 6.67% and is nearly two third of the threshold moisture content (<10%) which should be in a biomass suitable for pyrolysis. This result is comparable to the values for other lingo-cellulosic biomasses such as sugar cane leaves (5.67%) (Kumar et al., 2019b). The volatile matter content of the banana trunk was found to be 74.33%. The values of ash and fixed carbon content were found to be 11.67 and 7.33%, respectively. The values of carbon, hydrogen, nitrogen, and oxygen were found to be 33.09, 2.94, 0.94, and 63.03%, respectively. It was observed that the carbon content is lower than common agricultural residues like rice husk (35.58%), wheat straw (48.24%), sugar cane bagasse (46.19%), rice straw (55.79%), arhar stalk (36.19%) reported previously (Kumar et al., 2019c). The cellulose, hemicellulose and lignin contents were found to be 25, 25, and 15%, respectively. The higher heating value (HHV) was estimated to be 13.41MJ/kg.

From Table 7.1 it is seen that results of proximate and ultimate analyses, HHV and biological composition for banana leaves and leaves-briquettes, banana peel, banana pseudo-stem, and banana fruit-bunch stem are available in the published literature. The magnitudes of most of these parameters are nearly similar for various types of banana biomasses. The values obtained in this work also fall within the same range. Abdullah et al. (2019) and Selvarajoo et al. (2019) have reported the lowest values of fixed carbon (0.2 to 0.43%). The nitrogen content in various types of banana biomass has varied from 0.19 to 2.45% and sulphur from nil to 0.45%. The values of nitrogen content reported by Abdullah et al (2014), Kabenge et al (2018) and Kumar et al (2019) have varied from 1.87 to 2.45%. The highest sulphur level (0.45%) has been reported by sellin et al (2013) and Abdullah et al (2019).

There is a wide variation in the reported percentage of biological constituents-hemicelluloses (0.77 to 41.38%), cellulose (6 to 25%) and lignin (5 to 37.3%). The heating values reported by various workers are nearly of similar order and have varied from 12.70 to 17.20 MJ/kg. Such variations can primarily be due to the use of non-uniform and non-representative samples. Thus adequate care and strict adherence to the standard protocols is essential for obtaining reliable and reproducible results for thermochemical characteristics. In spite of these variations the thermo chemical characteristics, biological composition and calorific values indicate that the banana biomass likely to be a reasonably good fuel.

Table 7.1: Physicochemical properties of banana trunk/pseudo-stem, fruit-bunch stem, leaves, leaves-briquette, peel

Analyses	Present work	Peels (Selvarajoo et al., 2019)	Pseudo-stem (Abdullah et al., 2014)	Fruit-bunch-stem (Abdullah et al., 2014)	Pseudo-stem (Cheng et al., 2016)	Peel (Kumar et al., 2019)	Pseudo-stem (Sellin et al., 2013)	Peel (Kabenge et al., 2018)	Leaves (Kabenge et al., 2018)	Pseudo-stem (Kabenge et al., 2018)	Pseudo-stem (Nolasco et al., 1998)	Pseudo-stem (Guimarães et al., 2009)	Leaves briquette (De Oliveira Maia et al., 2014)
Proximate analysis (wt. %)													
Moisture content	6.67 ± 1.53	11.40	10.20	11.40	-	8.57	9.74	11.56	6.67	7.98	10-12	8.57	7.17
Volatile matter	74.33 ± 0.58	83.10	88.80	79.10	80.06	67.48	71.70	88.02	83.35	89.43	-	-	75.30
Ash content	11.67 ± 1.15	5.80	11.00	20.60	3.94	4.15	9.85	9.28	9.05	1.21	1-2	4.14	10.70
Fixed carbon	7.33 ± 0.25	0.43	0.20	0.30	16	19.80	18.45	2.70	7.60	9.36	-	-	14.00
Calorific value (HHV, MJ/kg)	13.41	-	15.50	12.70	17.61	18.52	14.10	16.15	17.37	15.04	-	-	17.70
Ultimate analysis (wt. %)													
C	33.09	-	37.93	35.58	47.98	45.24	37.69	35.65	38.57	33.46	-	-	46.80
H	2.94	-	4.46	4.62	5.50	5.78	5.58	6.19	6.44	6.44	-	-	6.03
N	0.94	-	1.87	2.19	0.61	2.28	0.19	1.94	2.45	0.80	-	-	0.80
O	63.03	-	55.37	57.16	41.30	36.26	46.39	45.94	43.49	49.94	-	-	37.90
S	-	-	0.37	0.45	0.10	0.37	0.30	0.003	0.003	-	-	-	0.30

H/C	1.07	-	1.41	1.56	1.37	1.53	1.77	0.17	2.00	2.30	-	-	1.55
O/C	1.43	-	1.09	1.20	0.87	0.60	0.92	0.96	0.84	1.11	-	-	0.60
Compositional analysis (wt. %)													
Hemicellulose	25.00 ± 0.61	-	17.50	27.80	-	-	-	41.38	23.46	25.36	6-8	0.77	-
Cellulose	25.00 ± 0.49	-	44.00	39.80	32.36	-	-	9.90	35.58	38.48	50.15	60-65	-
Lignin	15 ± 0.42	-	37.30	18.00	18.36	-	-	8.90	-	10.58	5-10	17.44	-

7.3.2 FTIR analysis

Functional groups of the organic compounds to identify the primary biomass constituents-cellulose, hemicellulose and lignin present in the banana trunk (BT) biomass, which control the thermal degradation behavior were determined using FTIR spectroscopy in the range of 500 to 4000cm^{-1} wave-numbers (Table 7.2). The peak at 3292cm^{-1} is due to the presence of O-H stretching of phenolic, water molecule, and alcoholic groups present in the cellulose and lignin chains (Mishra and Mohanty, 2018b). The peak at 2915cm^{-1} is due to the aliphatic CH, CH_2, and CH_3 stretching's of alkanes and also indicate the asymmetric and symmetric methyl group stretching's (Doshi et al., 2014; Eshun et al., 2017). The absorption band at 1643cm^{-1} is attributed to the carbonyl group of the hemicellulos and aromatic ring C-C, amine N-H, alkene C=C stretching's and phenyl ring C-H group substitution overtones due to cellulose, lignin and protein molecules present in the biomass (Mothé and De Miranda, 2009). The band at 1515cm^{-1} is due to the aromatic rings of lignin. The peak at 1373cm^{-1} is due to aromatic methoxy groups and that at 1334cm^{-1} indicates the presence of C-H and aliphatic C-H_2 in phenol (Mishra and Mohanty, 2018b). The bands at around 1254 to 1042cm^{-1} are due to the functional groups of carbohydrates of cellulose and hemicellulose. The peak observed at 1041$cm^{-1}$are due to the C-OH stretching vibrations (Mothé and De Miranda, 2009).Peaks between 450 and 900cm^{-1} indicate the presence of aromatic ring C-C stretching (Kumar et al., 2019c).

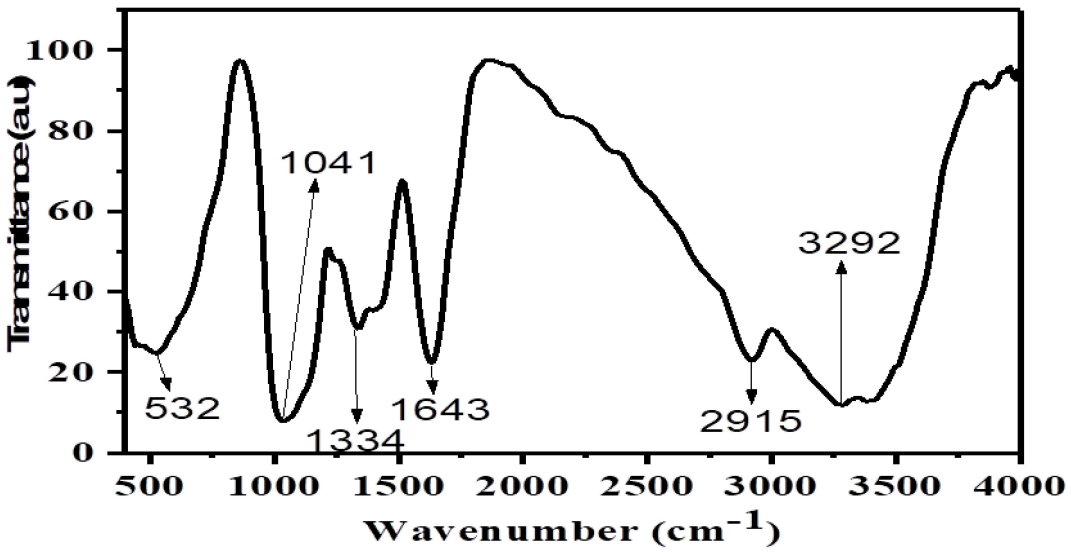

Fig.7.1 FTIR spectra of banana trunk biomass

Table 7.2: Major chemical groups present in banana pseudo-stem (or banana trunk) biomass

Wavenumber(cm-1)	Intensity	Responsible group	Contributing Molecule
3400	Strong	O-H stretching	Cellulose, hemicellulose, lignin, water
2920	Weak	C-H, C-H_2 and C-H_3 stretching	Cellulose, hemicellulose, lignin
1726	Shoulder	C=O stretching	Aliphatic carboxylic acids, ketone of hemicellulose
1635	Strong	O-H bending, C=C and Ar-C=O stretching	Water, lignin
1515	Very weak	C=C aromatic skeletal vibration	Lignin
1424	Medium	CH_2 deformation	Cellulose, hemicellulose, lignin
1373	Medium	CH_3 deformation of Ar-OCH_3, OH-deformation, O-H deformation (in plane)	Cellulose, hemicellulose, lignin
1254	Weak	C=O stretching	Cellulose and hemicellulose
		C=C stretching	Lignin
1156	Shoulder	C-O-C asymmetric stretching	Cellulose, hemicellulose, lignin
1106	Shoulder	Ar-C-H deformation	Lignin
1056	Strong	C-O stretching of COH	Cellulose, hemicellulose, lignin
1042	Strong	CO-C stretching	
894	Very weak	C-H deformation, Inorganic group vibrations	Cellulose, Inorganic compounds
774	Very weak	Ar-C-H out of plane vibration	Lignin

7.3.3 The TGA and DTG results

The thermal decomposition behavior of banana trunk biomass was studied using the TGA technique at the heating rates of 10, 15, 20, and 25°C/min in an inert atmosphere (N_2, flow 100mL/min) within the temperature range of ambient (30°C) to 800°C. These results are shown as %weight loss versus temperature (T, °C), derivative weight loss versus T, conversion (α) versus T and heat flow (mW/mg) versus T plots in Fig. 7.2 (a) through 7.2 (d), respectively. From Fig. 7.2 (a) through 7.2(c), it is seen that for the heating rate of 25°C/min the profiles of all three curves are clearly different from the corresponding curves for the heating rates of 10, 15 and 20°C. The curves for the highest heating rate (25°C/min) are exhibiting three distinct temperature zones- ambient to 150°C, 150 to 325°C and 325 to 800°C. In case of the lower three heating rates the curves are exhibiting four temperature zones- (i) ambient to 150°C, (ii) 150 to 325°C, (iii) 325 to 600°C (iv) 600 to 800°C. From Fig. 7.2 (a) and 7.2(c) it is seen that at all four heating rates the nature of curves is nearly similar. In the first temperature zone there is mild change in %weight loss, derivative weight loss and conversion. In this zone the weight loss of biomass is primarily due to the removal of moisture and some low molecular weight volatile compounds from the banana trunk biomass. It is also known as the initial drying stage. In the next temperature zone (150 to 325°C) also the nature of curves are similar but the slopes are much steeper indicating a faster change in conversion and %weight loss with increasing temperature. Primarily hemicellulose and cellulose degrade in this temperature zone. In the third temperature zone (325 to 600°C) the curves for the three lower heating rates show a less steep change in conversion and exhibit a point of inflection. This can be attributed to the increase in degradation of lignin and endothermic/exothermic interactions between various

degradation products. Several parallel reactions occur between the products formed leading to the formation of gaseous and liquid products. This stage is often called the active stage of pyrolysis. In the fourth temperature zone (600 to 800^{o}C), the %weight loss and conversion are nearly constant and it is characterized by the char formation as most of the char forms in this stage. At the highest heating rate (25^{o}C/min), there is a continuous slow change in %weight loss and conversion in the temperature range of 350 to 800^{o}C and the portion with inflection observed at lower heating rates is absent. This behaviour can be attributed to the increase in the formation of active species through the thermal degradation of cellulose, interaction amongst themselves and with lignin as well as gradual degradation of lignin leading to char formation. Abdulla et al (2014) and Kabenge et al (2018) observed similar behaviour for banana leaves and fruit-bunch stem, and banana peel and banana-stem, respectively. Guimarães et al (2009) obtained similar TGA-temperature profile for banana fiber.

Figure 7.2 (b) depicts plot of %weight change per minute versus temperature for all heating rates. All curves show a sharp peak in the center at around 325^{o}C with weak peaks on its either sides. It is also seen that as the heating rate decreases the sharpness of the central peak also decreases. In the first temperature zone (up to 150^{o}C) the peaks for lower heating rates are very weak but that for the highest heating rate it is relatively larger. In this zone mostly moisture and low molecular weight compounds are removed and there may be some interaction between them. At lower heating rates this removal takes place at a slower rate but at the highest heating rate most of lower molecular weight volatile compounds are removed relatively quickly. Being active they may also interact with each other and moisture quite quickly hence the %weight loss gets reduced and the peak height gets

increased. The central sharp peak at all heating rates is characterized by the rapid thermal degradation of most of hemicellulose and cellulose and some lignin. Since this process is highly dependent upon the heating rate, the peak height gets reduced with decreasing heating rate.

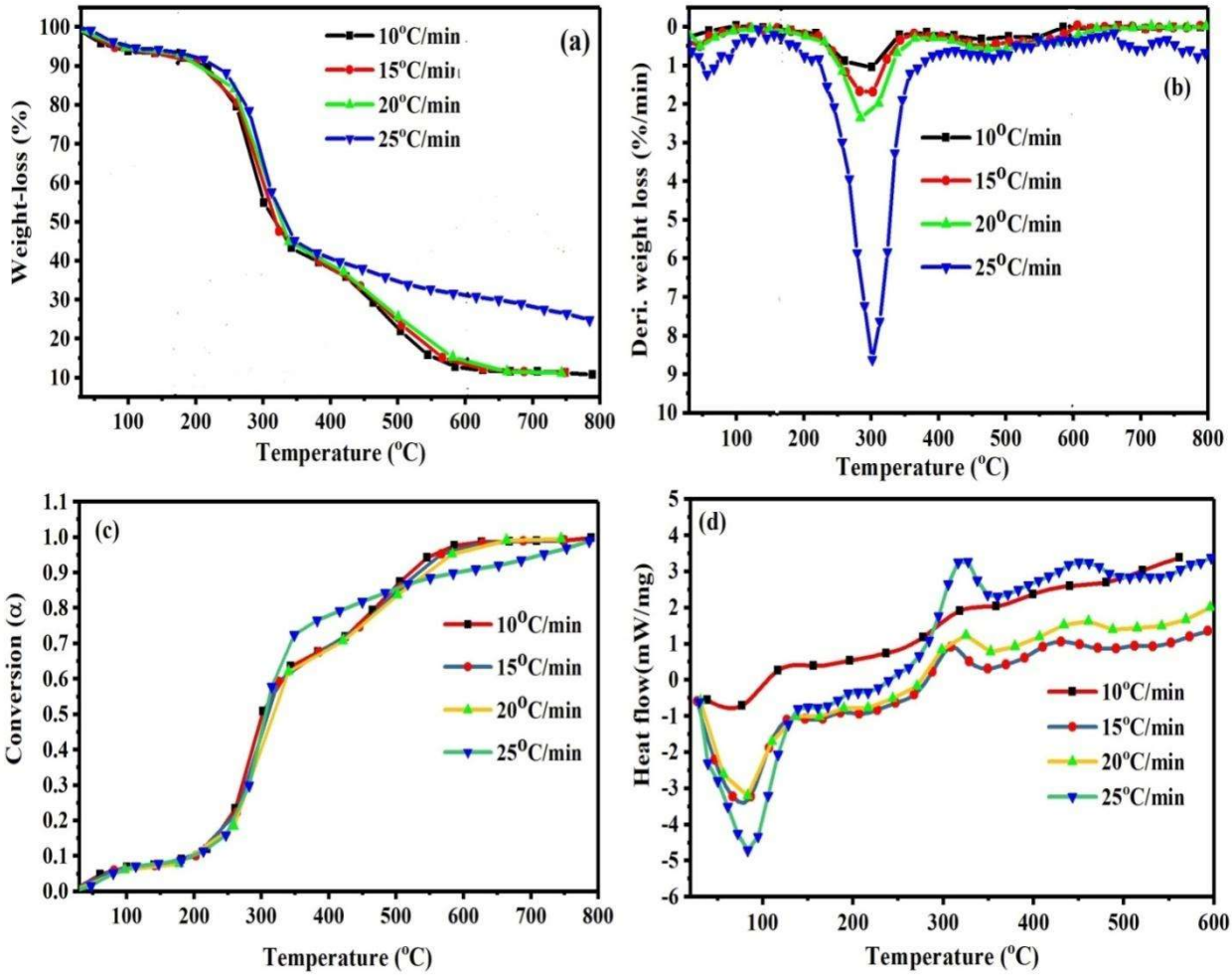

Fig. 7.2 Effect of heating rate on pyrolysis of banana trunk biomass: (a) TGA curves; (b) DTG curves; (c) Conversion (α); (d) DSC curves

The initial and final temperatures of each stage increase with the heating rate (Table 7.3). The percent weight loss decreases in the order of 7.10, 6.81, 6.29 and 5.99% at the heating

rates of 10, 15, 25 and 25°C/min, respectively in Stage I. In Stage II the weight loss decreases in the order 47.13% (at 10°C/min) > 46.21 (at 15°C/min) > 45.53% (at 20°C/min) > 43.05% (at 25°C/min) and this is attributed to the fact that in this stage at a higher heating rate, thermal resistance of particle lead to a temperature lag along the radial direction of the biomass particle (Cheng et al., 2016). Similar, trend of weight loss is also observed in Stage III as the weight loss decreases in the order 34.40% (at 10°C/min) > 33.34 (at 15°C/min) > 32.72% (at 20°C/min) > 27.06% (at 25°C/min). It is interesting to note that in the char formation stage (Stage IV) the corresponding variations in the percent weight losses are 2.00, 1.96 and 2.59% at the heating rates of 10, 15 and 20°C/min, respectively. The observed decrease in the percent weight loss with increasing heating rate may be due to the formation of larger amount of high molecular compounds and char.

The rate of maximum weight loss increased with heating rate and temperature in the order 1.23%/min at 283°C (10°C/min) < 1.68%/min at 301°C (15°C/min) < 2.36%/min at 302°C (20°C/min) < 8.62%/min at 302°C (25°C/min) (Fig.7.2 (b) and Table 7.3). The residual percentage weight (char) changed in the order of 10.54, 10.68, 10.87 and 23.90% at heating rates of 10, 15, 20 and 25°C/min, respectively. Hence, in order to reduce the char formation a lower heating rate (10°C/min) is favorable than the higher one (25°C/min) for the thermal decomposition of banana trunk biomass.

Figure 7.2 (c) shows the variation of conversion (α) with increasing temperature. It is observed that approximately 60% conversion of biomass gets completed at around ~350°C at each heating rate. In the temperature range of 350 to 600°C, the change in conversion is less steep and the conversion versus temperature plot shows a point of inflection and becomes nearly constant at around 90% after 600°C for the heating rates of 10, 15, and

20°C/min. The fluctuations in %weight loss versus temperature and conversion plots as observed in Fig 7.2 (a) and Fig. 7.2 (c), in the temperature range of 325 to 600°C at these heating rates may be attributed to the interactive endothermic/exothermic reactions occurring between the products of thermal degradation of biomass. At the highest heating rate of 25°C/min, the behaviour of %weight loss- and conversion-temperature profiles are distinctly different. This may be because of the poor heat transfer efficiency due to thermal resistance of biomass particles. Further, the release of volatile constituents and their secondary reactions with char being endothermic cause the absorption of heat before being transferred to the core of biomass particles causing reduction in the thermal degradation process (Cheng et al., 2016). It can be inferred that pyrolysis at moderate temperature, higher heating rate and shorter residence time will result in a higher bio-oil yield whereas low temperature, lower heating rate and longer residence time will give more char.

Table 7.3: TGA and DTG analysis of banana trunk biomass

Heating rate, β (^{o}C/min)	Initial Temperature T_i (^{o}C)	Final Temperature T_f (^{o}C)	Peak Temperature T_P (^{o}C)	-DTG_{max}(%/min)	Weight loss (%)
Stage I					
10	18.79	150	18.79	0.49	7.10
15	19.17	150	19.17	0.63	6.81
20	18.97	150	18.97	0.43	6.29
25	21.17	150	21.17	0.11	5.99
Stage II					
10	150	325	283	1.23	47.13
15	195	325	290	1.68	46.21
20	210	325	290	2.36	45.53
25	225	325	300	8.62	43.05
Stage III					
10	325	600	590	0.46	34.40
15	325	600	595	0.66	33.34
20	325	600	600	0.55	32.72
25	325	800	605	0.06	27.06
Stage IV					
10	600	800	607	0.10	2.00
15	600	800	609	0.08	1.96
20	600	800	610	0.31	2.59

7.3.4 Differential scanning calorimetric (DSC) results

Figure 7.2 (d) shows the effect of heating rate on the heat flow (mW/mg)-temperature profiles. It is seen that except for the heating rate of 10°C, the heat flow curves show an initial endothermic region up to 300 to 325°C. In case of the lowest heating rate (10°C/min) the endothermic behavior is exhibited only up to about 125°C. This is followed by an increasingly exothermic behavior at higher temperatures. However, in each case an endothermic peak has been observed at around 75 to 90°C and there is a gradual shift in the peak towards the higher temperature with increase in the heating rate. This can be attributed to the removal of moisture and some low molecular weight volatile compounds from the biomass sample due to thermal depolymerization of hexoses which involves the formation of volatiles, as indicated by the endothermic peaks. The DSC profile is in agreement with the TGA/DTG profiles. For temperatures above 300 to 325°C, the pyrolysis behaviour is predominantly exothermic. For the heating rate of 10°C/min, the exothermic behaviour is exhibited from 100°C onwards.

The observed exothermic behaviour exhibited beyond 300 to 325°C by the heat flow-temperature profile can be attributed to the combustion and exothermic char forming reactions. It has been reported that under char forming conditions the pyrolysis of cellulose is exothermic (Milosavljevic et al., 1996; Ridout et al., 2015; Soares et al., 1995; Yang, 2007). The pyrolysis of hemicellulose and lignin beyond 150°C is also reported to be exothermic in nature (Yang, 2007). For banana fibers Guimarães et al (2009) reported a peak at 300°C due to the decomposition of cellulose and peaks at 400-500°C due to the breaking of the bonds of lignin. The difference between present results and those of Guimarães et al (2009) may be due to use of dissimilar banana bio-masses.

7.3.5 Burnout temperature

The burnout temperature is the temperature at which the biomass is totally pyrolyzed and the loss due to thermal degradation is below 1.0% (Kumar et al., 2019c; Mishra and Mohanty, 2018c). The burnout temperature plays an important role in the selection of a biomass for pyrolysis and the design of the pyrolyser. A higher burnout temperature indicates presence of less thermally degradable fraction in the biomass(Lu, 2019). It was observed that the burnout temperature of banana trunk biomass increased with increasing heating rate. At the heating rates of 10, 15, 20, and 25°C/min it was found to be 325, 345, 360 and 363°C, respectively. This is in conformity with the observations reported previously by several other workers (Lu, 2019; Kumar et al., 2019c; Mishra and Mohanty, 2018c; Osman et al., 2017) for lingo-cellulosic biomasses. The increase in the burnout temperature with heating rate can be attributed to higher coking and char formation at higher heating rates.

7.3.6 Iso-conversional kinetic analysis

The activation energy, E_α and pre-exponential factor, A were evaluated from the non-isothermal TGA data using various iso-conversional models. In case of FWO, Starink, KAS and Tang iso-conversional models, the values of E_α were calculated from the slopes of the linear plots prepared using respective models at $\alpha = 0.1$ to 0.9 (Fig. 7.3) and using the advanced iso-conversional models of Vyzovkin and Vyzovkin AIC by minimizing their corresponding functions (Dhyani et al., 2017; Mishra et al., 2014). The values of E_α and A, obtained using all six models for $\alpha = 0.1$ to 0.9 are presented in Table 7.4. It is interesting to note that the lowest average activation energy was found to be 292.78kJ/mol using

Vyzovkin AIC model. The calculated average activation energy decreased in the order FWO > KAS > Vyzovkin > Starink >Tang > Vyzovkin AIC. He et al (2018), and Damartzis et al (2011) observed similar trend for coal and cardoon leaves pyrolysis, respectively.

For conversion (α) up to 0.2 activation energy is energy required for the removal of moisture and light components from the banana trunk biomass sample and initiation of pyrolysis reactions. Figure 7.4 depicts the variation of calculated activation energy with conversion (> 0.2) for various models. For the conversion range of 0.2 to 0.3, the values of activation energy obtained using FWO; KAS and Vyzovkin models are more or less constant while those obtained with Starink, Tang and Vyazovkin AIC models are changing. In the conversion range of 0.3 to 0.5 it increases from 282.80 to 409.91, 288.73 to 422.09, 288.36 to 421.69, 288.43 to 421.59, 284 to 417 and 178 to 257kJ/mol while in the range of 0.6 to 0.8 it increases from 563.55 to 555.20, 478.24 to 489.60, 484.24 to 573.15, 477.67 to 489.04, 473 to 566 and 258 to 535kJ/mol, respectively for FWO, Starink, KAS, Tang, Vyzovkin and Vyzovkin AIC models. This increase in the activation energy from the conversion level of 0.3 to 0.5 is approximately 12% and can be ascribed to the degradation of hemicellulose and cellulose. For α = 0.6 to 0.8, the values of activation energy increase by 14 %.The higher activation energy in this range is attributed to the decomposition of lignin.

The thermal conversion of the bulk organic fractions of the biomass is a temperature dependent phenomenon. Therefore, as the temperature increases the conversion (α) increases and consequently the activation energy also changes. For banana peels, Kumar et al (2019) reported the average activation energy values as 108.42, 167.64, 157.42, 181.27

and 201 kJ/mol using Kissinger, KAS, FWO, Friedman and Coats–Redfern models. Cheng et al (2016) investigated pyrolysis of banana stem and used the method of Coats-Redfern. They found the values of activation energy to be in the range of 130.63–192.10 kJ/mol and a pre-exponential factor range of $2.42\times10^{7} – 4.10 \times 10^{10} s^{-1}$.

The KAS and Vyzovkin models show similar variations in the activation energy with conversion due to the use of similar basic approach. The Starink and Tang models are based on similar mathematical approximations and exhibit nearly identical behaviour. Vyzovkin and Vyzovkin AIC models do not utilize any mathematical assumptions among all the six models used for analyzing the TGA data. Therefore these two models are more appropriate for the analysis of biomass pyrolysis because no approximation errors are involved. The Vyzovkin AIC is the advanced version of Vyzovkin model and it pronounced the accuracy of the same by taking the smaller values of $\Delta\alpha$ (Kumar et al., 2019b).

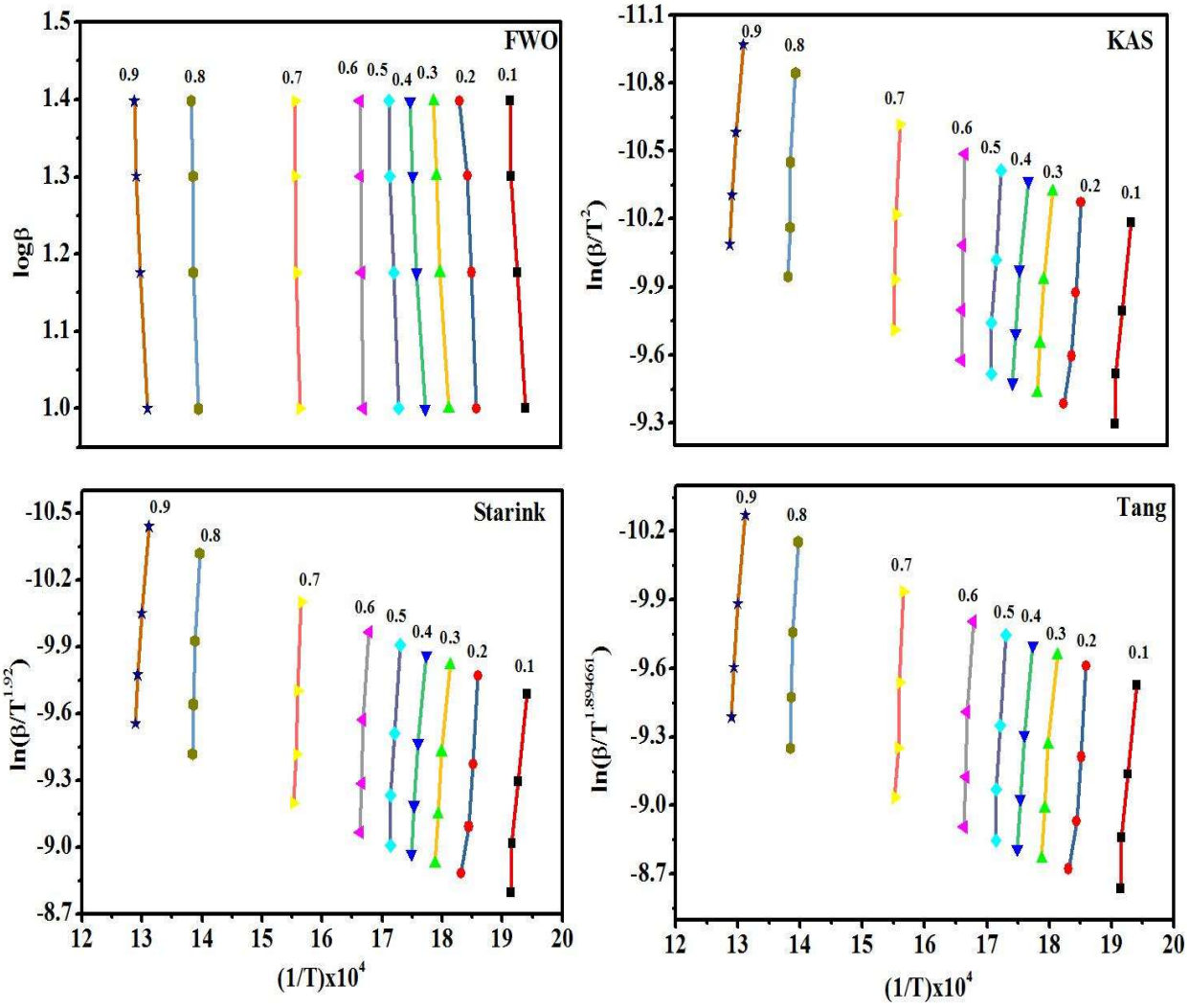

Fig. 7.3 Arrhenius plots for activation energy calculation using different iso-conversional models

There are some limitations in the generalization of the estimation of kinetic and thermodynamic parameters through the thermal kinetic analysis because activation energy is a temperature dependent variable and each biomass has its own decomposition temperature. Further, the composition of the same type of biomass, particularly the mineral matter content, will depend upon the nature of soil and the climatic conditions where it has

been grown. Kumar et al. (2019) through their experiments on pyrolysis of Ru and Fe impregnated banana pseudo-stem biomass have already shown that presence of metal results in lowering of the activation energy. Thus the mineral matters present in biomass have a positive influence on biomass pyrolysis. Therefore, variation in activation energy with the nature of biomass or for the same biomass obtained from different geographical locations is possible. Further, the experimental conditions (such as particle size and size distribution, biomass morphology, heating rate, surrounding atmosphere, material of construction of crucible, type of sensor) employed and the mathematical models used will also affect the estimated values (Kumar et al., 2020a).

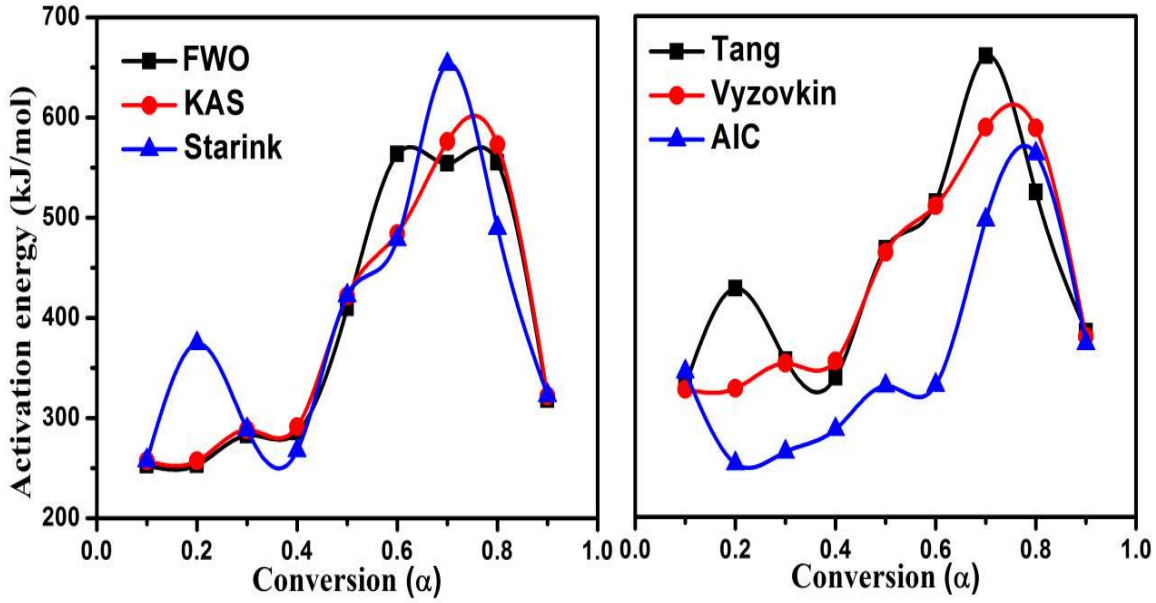

Fig. 7.4 Activation energy versus conversion plots for different iso-conversional models

7.3.7 Thermodynamic parameters

The values of pre-exponential factor (A) and thermodynamic parameters such as change in enthalpy (ΔH), change in Gibbs free energy (ΔG) and change in entropy (ΔS) calculated using all six models are reported in Table 7.4. The average values of change in enthalpy using Vyzovkin AIC model is the lowest (287.73kJ/mol) and for all other models it has varied between 374.62 to 389.88kJ/mol. It is seen that the difference between values of E_α and ΔH at each conversion level is very small (~5kJ/mol), from which it can be inferred that the pyrolysis of banana trunk biomass for energy generation is viable.

In the conversion range of 0.1 to 0.9, the values of ΔG calculated using FWO, Starink, KAS, and Tang models vary nearly within the same range (from 148 to 225kJ/mol). The change in entropy (ΔS) is related to the degree of randomness and formation of wide types of new species due to the thermal pyrolysis of a solid biomass like banana trunk. The calculated values of ΔS at each conversion (α) level using all six kinetic models are reported in Table 4.The average values of ΔS are found to be 336.33, 354.40, 175.01, 353.65, 394.36 and 235.45J/mol.K for FWO, Starink, KAS, Tang, Vyzovkin and Vyzovkin AIC models, respectively. The positive values of ΔS indicate that the degree of randomness of BT biomass constituents is higher than those for the thermal degradation products. The knowledge of thermodynamic parameters is likely to be helpful in designing gasifier and pyrolyser and for carrying out the energy balance. It must be emphasized here that for design purposes gasification/pyrolysis experiments using bench scale reactors are

necessary. However, the results obtained through TGA/DTG/DSC experiments will be useful in carrying out such experiments.

Table 7.4: Kinetics and thermodynamic parameters of banana trunk pyrolysis

α	E_α (kJ/mol)	A (min^{-1})	ΔH (kJ/mol)	ΔG (kJ/mol)	ΔS (J/mol.K)	E_α (kJ/mol)	A (min^{-1})	ΔH (kJ/mol)	ΔG (kJ/mol)	ΔS (J/mol.K)	E_α (kJ/mol)	A (min^{-1})	ΔH (kJ/mol)	ΔG (kJ/mol)	ΔS (J/mol.K)
			FWO					**Starink**					**KAS**		
0.1	252.79	4.0×10^{23}	248.50	148.12	194.85	257.72	1.3×10^{24}	253.44	148.03	204.59	257.37	1.2×10^{24}	253.08	148.04	148.04
0.2	253.17	3.4×10^{22}	248.70	155.19	173.86	374.52	3.1×10^{34}	370.05	153.44	402.76	257.38	8.9×10^{22}	252.91	155.12	155.12
0.3	282.80	5.7×10^{24}	278.22	158.98	216.21	288.73	2.1×10^{25}	284.14	158.88	227.12	288.36	1.9×10^{25}	283.78	158.89	158.89
0.4	285.93	2.8×10^{24}	281.24	162.79	210.10	267.49	5.1×10^{22}	262.80	163.10	176.83	291.44	9.2×10^{24}	286.75	162.70	162.70
0.5	409.91	1.3×10^{35}	405.12	165.53	414.46	422.09	1.8×10^{36}	417.28	165.39	435.77	421.69	1.6×10^{36}	416.89	165.39	165.39
0.6	563.55	3.9×10^{47}	558.59	169.53	652.86	478.24	1.1×10^{40}	473.29	170.34	508.35	484.24	3.8×10^{40}	479.29	170.28	170.28
0.7	554.27	2.8×10^{43}	548.96	182.91	573.06	653.25	4.2×10^{51}	647.94	182.03	729.38	576.24	1.8×10^{45}	570.92	182.70	182.70
0.8	555.20	3.4×10^{38}	549.25	207.09	477.77	489.6	4.9×10^{33}	483.65	207.84	385.12	573.15	7.1×10^{39}	567.20	206.90	206.90
0.9	318.28	3.5×10^{19}	311.94	225.16	113.84	322.64	7.1×10^{19}	316.30	225.07	119.68	322.13	6.5×10^{19}	315.79	225.08	225.08
Avg.	**386.21**	**4.4×10^{46}**	**381.17**	**175.03**	**336.33**	**355.43**	**4.7×10^{31}**	**389.88**	**174.91**	**354.40**	**385.77**	**2.1×10^{44}**	**380.73**	**175.01**	**175.01**

			Tang					Vyzovkin					Vyzovkin AIC		
0.1	257.45	1.2×10^{24}	253.17	148.04	204.06	253	1.1×10^{22}	248.72	157.40	164.54	274	1.1×10^{24}	269.72	157.03	203.04
0.2	374.09	2.8×10^{34}	369.62	153.45	401.95	254	1.3×10^{22}	249.53	157.38	166.04	164	2.9×10^{13}	159.53	159.40	0.24
0.3	288.43	1.9×10^{25}	283.84	158.89	226.57	284	9.9×10^{24}	279.41	156.86	220.82	178	6.6×10^{14}	173.41	159.02	25.94
0.4	267.22	4.8×10^{22}	262.53	163.11	176.34	287	1.9×10^{25}	282.31	156.81	226.12	205	2.6×10^{17}	200.31	158.37	75.58
0.5	421.59	1.6×10^{36}	416.78	165.39	434.89	417	4.8×10^{37}	412.19	155.09	463.25	257	2.6×10^{22}	252.19	157.32	170.94
0.6	477.67	9.9×10^{39}	472.72	170.35	507.38	473	1.0×10^{43}	468.05	154.51	564.93	258	3.2×10^{22}	253.05	157.30	172.50
0.7	652.43	3.6×10^{51}	647.12	182.04	728.08	567	8.6×10^{51}	561.69	153.67	735.17	456	2.5×10^{41}	450.69	154.68	533.36
0.8	489.04	4.5×10^{33}	483.08	207.85	384.33	566	6.9×10^{51}	560.05	153.68	732.19	535	7.9×10^{48}	529.05	153.94	675.88
0.9	322.33	6.8×10^{19}	315.99	225.07	119.27	316	1.1×10^{28}	309.66	156.37	276.20	308	1.9×10^{27}	301.67	156.49	261.58
Avg.	**355.03**	**4.0×10^{37}**	**389.43**	**174.91**	**353.65**	**379.67**	**1.7×10^{51}**	**374.62**	**155.75**	**394.36**	**292.78**	**8.7×10^{47}**	**287.73**	**157.06**	**235.45**

7.3.8 Reaction mechanism

Comparison of experimental and theoretical z-master z (α) versus conversion plots is a convenient way of discerning the reaction mechanism of biomass pyrolysis (Criado et al., 1989). Equation (4.54) has been used for plotting the theoretical z-master curves using the algebraic equations for g (α) and f (α) listed in Table 4.2. Equation (4.56) has been used to prepare the experimental z (α) curve using the values of activation energy calculated through Vyzovkin AIC model. The experimental and theoretical curves are depicted in Fig 7.5. It is seen that up to α = 0.3, the experimental z (α) curve is overlapping with the z-master curve for A_2 applicable for the nucleation and growth mechanism, Zhouling et al (2009) also observed a similar behaviour for cotton stalk. For α = 0.3 to 0.85, the experimental curve crosses over most of the theoretical curves representing different reaction mechanisms for different values of conversion. Hence, it can be inferred that the thermal degradation of banana trunk biomass involves a complex reaction mechanism. Over very narrow ranges of conversions levels within the conversion range of 0.3 to 0.85 the experimental curve follows the theoretical curve for A_4 (nucleation and growth), R_3 (phase boundary-controlled reaction, contracting volume), A_3 (nucleation and growth), R_2 (phase boundary-controlled reaction, contracting area). Thus it is difficult to clearly elucidate the reaction mechanism for thermal degradation of BT biomass using a single reaction mechanism in this range, however, over the conversion range of 0.1 to 0.35, the banana trunk biomass degrades following the nucleation and growth and phase boundary controlled reactions. For this conversion range Kumar et.al (2019b, 2020a) arrived at similar conclusions for sugar cane leaves (Kumar et al., 2019b) and rice husk Kumar et al (2020a).

As mentioned before pyrolysis and pyrolysis products are affected by particle characteristics, nature of biomass (pure and mixed), moisture content, mineral matter, heating rate, and catalysts. Thus the observed differences in the values of kinetic and thermodynamic parameters as well as prevailing reaction mechanism as reported by various workers even for the same biomass may be primarily due to the differences in above mentioned factors. Unfortunately most of the workers do not report sufficient information on many of these parameters. For a better inter comparison between the results of various workers these details should be reported.

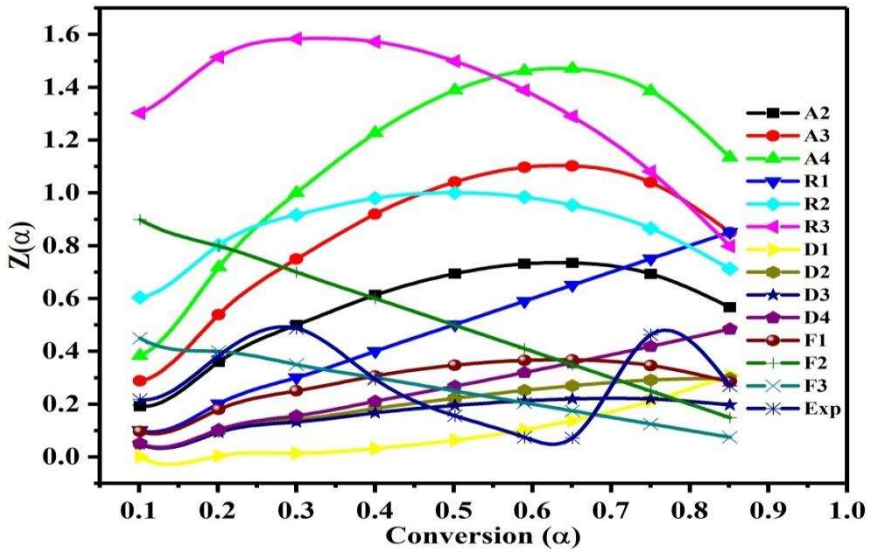

Fig. 7.5 Comparison of theoretical Z (α) versus conversion plots with experimental results

7.4 Conclusion

The banana trunk (or pseudo-stem) biomass is likely to be a reasonably good fuel. Its higher heating value (HHV) is 12.7 MJ/kg that is very close to that of the biomasses from other parts of banana including banana fruit peels (13.41 to 17.20MJ/kg). Pyrolysis of banana trunk takes place in four distinct sages that depend upon the heating rate with maximum weight loss occurring in the second stage. The activation energy increases with

conversion (α) irrespective of the iso-conversional model used. The small difference between activation energy and change in enthalpy (≈ 5 kJ/mol) indicates feasibility of pyrolysis. The pyrolysis follows the nucleation, growth and phase boundary mechanism.